Domain Dynamics in Thin Solid Films Following Ultrashort Pulse Excitation

Jesse J. Dean, David W. Rench, Nitin Samarth, and Henry M. van Driel

Phys. Rev. Lett. **111**, 035701 — Published 17 July 2013

DOI: 10.1103/PhysRevLett.111.035701

Domain Dynamics in Thin Solid Films Following Ultrashort Pulse Excitation

Jesse J. Dean[1], David W. Rench[2], Nitin Samarth[2], Henry M. van Driel[1*]

[1]*Department of Physics and Institute for Optical Sciences*
University of Toronto
Toronto, M5S1A7, Canada
[2]*Department of Physics and Materials Research Institute*
Pennsylvania State University
University Park, PA, 16802-6300, USA

Abstract

MnAs epilayers grown on GaAs are used as a model system to study the effects of strain and epitaxial constraints on the dynamics of structural domains following 150 fs pulse pumping. Optical diffraction over seven orders of magnitude of time is used to probe the evolution of the domains that are spatially periodic between 10 and 42 °C because of misfit strain and substrate mediated periodic elastic strain. Following excitation of 150 and 190 nm thick films, the domain fractions and the elastic strain oscillate with an ~ 400 ps period while the average low temperature phase fraction decreases monotonically for ~ 2 ns reflecting MnAs heat diffusion. Equilibrium structures are restored in 100 ns – 2 μs via substrate heat diffusion. Excitation of transient periodic domains from the homogeneous low temperature phase can occur for temperatures as low as 4 °C but only after ~ 20 ns during film cooling.

PACS numbers: 78.47.D-, 77.55.Nv, 68.60.-p, 64.70.Nd

Epitaxial thin solid films are not only of fundamental interest but they have also been at the heart of many technological advances because of their unique ferroelectric [1,2], ferromagnetic [3,4], and superconducting [5] properties. In many films lattice mismatch (misfit strain) between film and substrate over a certain temperature range leads to the development of elastic strain and unusual phase diagrams with multi-domains or coexisting phases [1,7-10] not found in the bulk materials. Additional functionalities for these films will emerge with improved understanding of how the mechanical epitaxial constraints influence the non-equilibrium dynamics and thermodynamic response of these domains, particularly on the nanoscale. We consider MnAs thin films grown on GaAs as a prototypical system to provide insight into the domain dynamics.

Bulk MnAs undergoes a first order magneto-structural transition from a paramagnetic β-phase (D_{2h} orthorhombic symmetry) to a ferromagnetic α–phase (D_{6h} hexagonal symmetry) upon cooling through 40 °C with an abrupt ~ 1% increase in a lattice constant [11,12]. MnAs thin films can be grown epitaxially on lattice-matched silicon or GaAs at high temperatures. When such films are cooled below 40 °C the film's lateral expansion is inhibited. Self-assembled, spatially periodic α, β phases emerge for temperatures in the range ~($10 < T_0 < 40$ °C) reflecting the balance between the release of free energy and the development of periodic elastic strain energy [3,13-16]. The α-phase fraction, ξ, decreases monotonically within the coexistence phase, and linearly with T_0 for ~$15 < T_0 < 36$ °C within which the fundamental period, Λ, of the stripes is independent of T_0 and related to mean film thickness, d_0, by $\Lambda \approx 4.8 d_0$ [14]. The spatial periodicity makes these domains ideal candidates for dynamical studies using diffraction techniques.

We report optical diffraction from MnAs ($\bar{1}100$)/GaAs (001) films at $4 < T_0 < 36$ °C following ultrashort pulse excitation. We show that epitaxial constraints cause the elastic strain to

oscillate during misfit strain reduction due to heat diffusion on a nanosecond timescale, much longer than the < 5 ps time associated with numerous types of ultrafast phase transitions in bulk materials [17-24] where *intrinsic* parameters govern the thermodynamic response. Transient periodic structures can be created from the homogenous α–phase only if T_0 is within a few degrees of 10 °C, and only while MnAs is cooling. We focus here on the MnAs structural, and not the magnetic, characteristics since strain is the common and dominant factor in the development of multi-domains in many thin film systems [7-10]; our optical diffraction experiments are also not directly sensitive to magnetization.

For our work two MnAs films were grown on a 360 μm thick (001) GaAs substrate using an EPI 930 MBE chamber; care was taken to ensure that Type A MnAs films were obtained [14]. During the optical experiments the sample temperature was controlled using a Peltier cooler and measured with a thermocouple. Because MnAs is reactive, during measurements samples were enclosed in a chamber containing dry nitrogen; they were otherwise stored under vacuum. The film thickness was measured to be d_0 = 150 ± 5 nm and 190 ± 5 nm using cross-sectional scanning electron microscopy. The surface structure was obtained using magnetic force (MFM) and atomic force microscopy (AFM). An AFM image of the 190 nm thick MnAs film is shown in Fig. 1(a) for T_0 = 22 °C and is similar to those of others [14]. MFM images reveal similar but less clear features. Analysis of the AFM image gives Λ = 1000 ± 100 nm (740 ± 70 nm) for the 190 (150) nm films with surface height modulation of ~3 nm. As also reported elsewhere [14-16], stripe irregularities, including bifurcations and width fluctuations, are present accounting for the range of Λ .

Sridhar *et al.* [7,8] and Roytburg [9,10] have modeled the spatially varying strain in a system consisting of a film with thickness d_0, composed of two striped structural domains with period Λ and phase fraction ξ, attached coherently to a thick substrate. The local strain (tensor) is

considered to be the sum of misfit and elastic strains. The difference in lattice constants between the two domains and substrate, if the film is detached from the substrate and free to expand, is represented by two misfit strains. The lateral constraints that occur when film and substrate are coherently contacted lead to periodic elastic strain throughout the system. The total strain field can be Fourier analyzed into components with period $q(2\pi/\Lambda)$, where $q=1,2,3\ldots$; the amplitudes are determined from mechanical equilibrium and stress boundary conditions. Minimization of the Helmholtz free energy determines Λ and the Fourier amplitudes as a function of d_0. Neglecting magnetic and elastic anisotropy effects, Kaganer *et al*. [13] have applied this analysis to the MnAs ($\bar{1}$100)/GaAs (001) system, in which the α-phase misfit strain (perpendicular to the stripes) is ~0.01 at T_0 = 40 °C and increases with decreasing T_0; insignificant misfit strain exists in the β-phase. The calculated Λ and ξ as a function of T_0 agree with experiment. Regions of large compressive (dilatational) elastic strain are associated with the β (α) phase. The q^{th} Fourier element of the surface height modulation is of the form $d_q = a_q(-1)^q q^{-1} sin(q\pi\xi)cos(2\pi qx/\Lambda)$ where x is the distance perpendicular to the stripes and a_q depends on d_0, Poisson's ratio and the misfit strain. Because α and β phases have slightly different refractive indices [25], a refractive index grating also exists that can be similarly Fourier decomposed, with the amplitude of the q^{th} component similarly $\propto q^{-1} sin(q\pi\xi)$. The MnAs surface can therefore be regarded theoretically as a superposition of amplitude and phase gratings. To first order in grating amplitude, probe light of wavelength λ incident at angle θ diffracts [26] at an angle θ_n given by $sin(\theta_n) = sin(\theta) + n\frac{\lambda}{\Lambda}$, with $\left|sin(\theta_q)\right| \le 1$ and $n = \pm 1, \pm 2, \ldots$. The n^{th} order diffracted field strength is $\propto n^{-1} sin(n\pi\xi)$, with intensity $\propto n^{-2} sin^2(n\pi\xi)$.

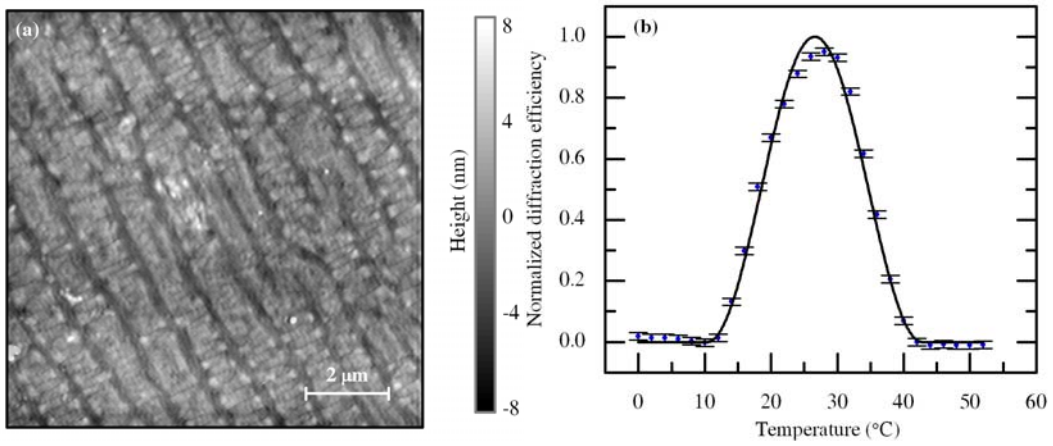

FIG 1. (a) AFM image of 190 nm thick MnAs on (001) GaAs at T_0 = 22 °C; light regions indicate α-MnAs where the surface is higher. (b) Temperature dependent diffraction (δ) at 387 nm; the solid curve represents a fitted $\sin^2(\pi\xi)$.

Our diffraction experiments employ 1 kHz repetition rate, 775 nm, 150 fs pump pulses. The p-polarized Gaussian profile pulses incident at 45° produced a 450x310 μm^2 spot (full width at half intensity maximum) with peak fluence of $\Phi = 1.05$ or $2\Phi = 2.1$ mJcm^{-2}. The $\lambda = 387$ nm, s-polarized 150 fs probe pulses, derived from a 775 nm beam, were incident on the pump spot center at $\theta = -45°$ with a 60x50 μm^2 spot size; spatial overlap was monitored at all probe-pump delays, τ, using a camera. Both pump and probe pulses have a characteristic absorption depth [25,27] of ~18 nm. First order diffracted light (n = -1) was collected from the films over an angular spectrum (related to variations in Λ) of θ_1 = -18°± 5° (-10°± 5°) using a photomultiplier tube behind a 7 cm focal length lens. A scattered light background, related to sample imperfections, exists for all temperatures and angles and has an intensity at/near the diffraction angle < 30% of the peak diffraction signal at T_0 ~ 26 °C.

We first consider the diffraction in the absence of the pump beam for 0 < T_0 < 55 °C. Hysteresis of ~5 °C is observed during heating/cooling cycles; only cooling data is shown here. After a temperature-independent scattered light background intensity was subtracted, the diffraction signal was fitted to $A \sin^2(\pi\xi)$ with ξ assumed to decrease linearly with T_0; best fit leads to an

effective coexistence phase range of 10-42 °C. The signal was normalized by its fitted peak value and Fig. 1(b) shows this normalized diffraction efficiency, δ, for the 190 nm film and the fitted $sin^2(\pi\xi)$ as a function of T_0. The maximum *absolute* diffraction efficiency, $(4\pm1)\,x10^{-5}$, is consistent with the 3 nm surface height modulation, the refractive index difference [25] between α and β phases and the phase difference of diffracted fields from the height and refractive index gratings. From the grating equation above, the only other diffraction order allowed is 2nd order ($n = -2$), but we were not able to detect this peak, and given the height and Λ fluctuations [14,16], *coherent* $q \neq 1$ gratings are likely weak, if not entirely absent, on MnAs.

For the time resolved diffraction we consider three time delay ranges: $0.15 < \tau < 18$ ps, 0.15 ps $< \tau <$ 5 ns and 10 ns $< \tau <$ 2 μs.

Regime I: 0.15 < τ < 18 ps. Figure 2(a) shows δ after 2Φ excitation of the 190 nm film at T_0 = 16, 20 and 32 °C; the 150 nm film gives similar results. Although δ is small for T_0 = 16 °C, consistent with Fig. 1(b), and increases only slightly, δ clearly increases in ~ 5 ps for T_0 = 20 and 32 °C. For T_0 = 32 °C if the film followed strictly thermal equilibrium behavior δ should *decrease* with increasing τ (see Fig.1(b)). We suggest that the δ variation here is related to induced changes in the refractive index grating, with negligible change in the surface corrugation, which depends on the strain field *throughout* the film [6,13] as seen below. Similar results are obtained for Φ fluence although the increase in δ is smaller. The 5 ps timescale is consistent with electron-lattice thermalization and associated changes to optical properties observed in bulk solids following ultrashort pulse excitation [17-24]. For $\tau >>$ 5 ps one can assume that a local lattice temperature can be defined.

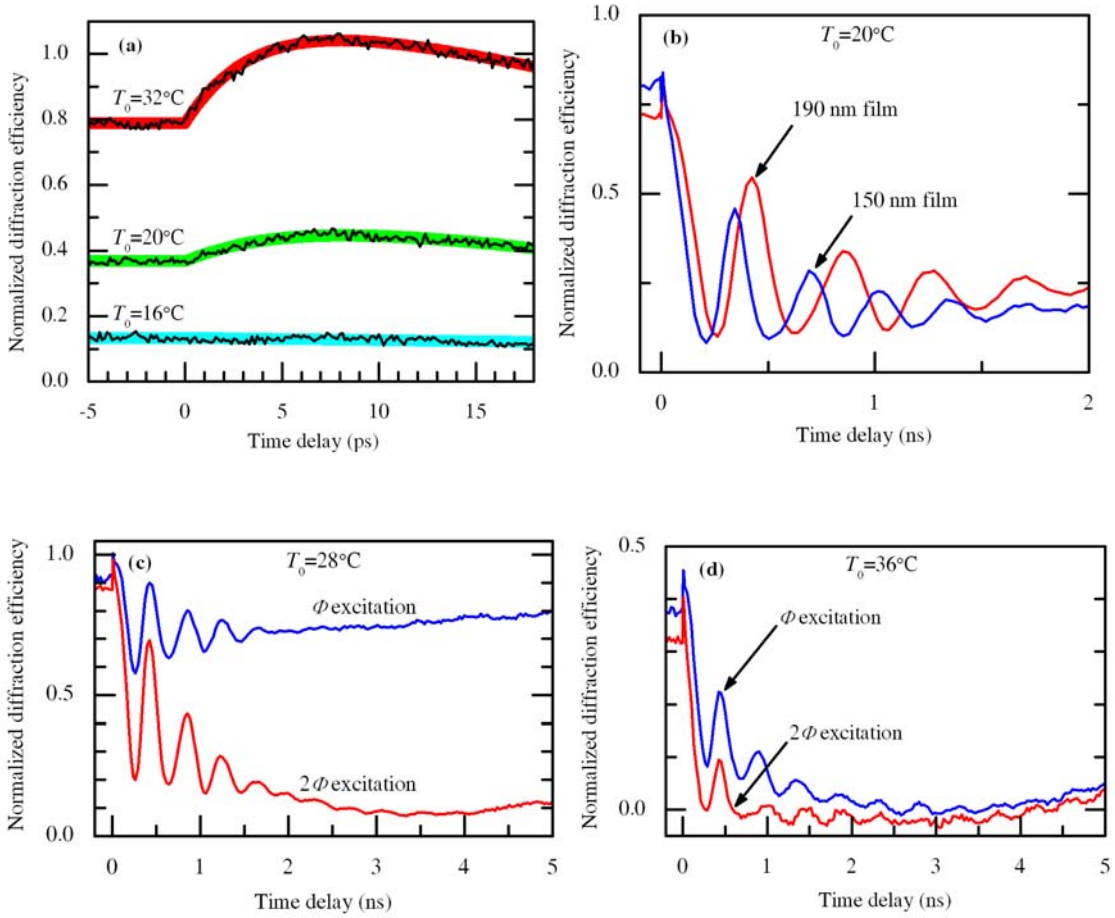

FIG. 2 (color online). (a) Time dependent δ of a 190 nm thick film at different temperatures for a 2Φ pump pulse. (b) Time dependent δ for 150 and 190 nm films at 20 °C for a 2Φ pump pulse. (c) Time-dependent δ for the 150 nm film at T_0 = 28 °C for two different pump fluences; (d) same with T_0 = 36 °C. Note that δ may fall slightly below zero at certain delays due to changes in the background scattered light level under film excitation.

Regime II: *0.15 ps* < τ < *5 ns*. Fig. 2(b) shows $\delta(\tau)$ following 2Φ excitation of the 150 and 190 nm films at T_0 = 20 °C. Figs. 2(c) and (2d) display $\delta(\tau)$ for the 150 nm film at T_0 = 28 and 36 °C excited at Φ and 2Φ, related results are obtained for the 190 nm film. In all cases, while slowly trending downward in ~ 2 ns, δ oscillates with a *constant* period of τ_p ~335± 4 (408± 4) ps for the 150 (190) nm film, although the amplitude depends on T_0 and pump fluence. For both films

Λ/τ_p equals 2300 ± 400 ms^{-1}, between the speeds of longitudinal (2500 ms^{-1}) and transverse (1600 ms^{-1}) elastic waves propagating along the Γ–M direction (*i.e.*, normal to the stripes) in *bulk* MnAs [28]. Since $d_0 < \Lambda$ interface effects may influence the elastic wave characteristics. We suggest that optically induced heating alters the misfit strain and the film's mechanical constraints, initially near the surface, inducing oscillations in the periodic elastic strain, local values of ξ, and hence surface corrugation [29]. Although low amplitude, laser-*induced* ultrasonic waves are well-known [30, 31], here the release of *pre-existing and large amplitude* (~0.01) periodic strain fields associated with different lattice structures induce temporal oscillation of α,β *phases*. The ξ oscillation is also governed not by local properties but by changes in the misfit strain throughout a region of the film.

We propose that the downward trend in δ observed in Figs. 2 (b)-(d) reflects reduction in the α–misfit strain with increasing depth as heat diffuses, thereby reducing the effective ξ and the amplitude of the surface corrugation. However, a model for a time- and spatially-dependent inhomogneous strain field requires extensive knowledge of how deposited optical energy is transformed and evolves during a phase transition and how strain evolves in response to these thermodynamics effects. This is beyond the scope of this Letter. Nonetheless, to provide some insight, using the MnAs latent heat [12,32], specific heat capacity [33] and specular reflectivity [25,27], we *estimate* that a 2Φ pump pulse induces the surface temperature to initially increase between 40 and 100 °C, depending on T_0, the latent heat release time, the energy deposition depth [34], etc. With heat diffusion the mean value of ξ and δ then decrease. For the MnAs heat diffusivity, $\kappa = 6.5\times10^{-7}$ m^2s^{-1} [32], at $\tau = 2$ ns the characteristic heat diffusion length $2\sqrt{\kappa\tau}$ is ~ 70 nm, a significant fraction of d_0. Hence non-oscillatory domain transformation can be expected on a nanosecond time scale. As seen in Figs. 2(b) and (c) δ never vanishes for T_0 = 20 or 28 °C and the entire film is never completely transformed to the β-phase. For T_0 = 36 °C, by ~ 2 ns complete film

transformation apparently occurs, limited by our knowledge of the scattered light background level within the coexistence phase. Since a 1-D heat diffusion calculation indicates that for $\tau = 2$ ns the MnAs/GaAs interface temperature rise is < 2 °C, the spatial period may also increase and become ill-defined [13,14] as the interface temperature approaches 40 °C. Finally, we note that for T_0 = 8 °C (MnAs initially in the α-phase), no diffraction is observed (not shown) and hence no regions of the film possess a coexistence phase with $\Lambda \sim 1000$ nm for $\tau < 2$ ns.

While our 1st order diffraction experiments obviously do not measure dynamics of the *complete* domain structure, they do monitor the phase fraction ξ through $sin^2(\pi\xi)$. If higher order domain Fourier components were accessible the associated elastic wave oscillation would occur at a higher frequency. However the downward trend of δ and ξ would likely still occur in ~ 2 ns since this time reflects reduction in the misfit strain as heat diffuses.

Regime III: $10\ ns < \tau < 2\mu s$. To study domain regrowth we used a continuous 409 nm probe beam; the photomultiplier/oscilloscope detection system limits time resolution to ~10 ns. Fig. 3 shows $\delta(\tau)$ for $\tau < 2$ μs for the 150 nm film at T_0 = 8, 16, 24 and 36 °C with a 2Φ pump incident; the 190 nm film gives similar results. As with domain erasure, regrowth depends on T_0 and pump fluence. The GaAs heat diffusivity [35], 3.1×10^{-5} m^2s^{-1}, is much larger than that of MnAs and a straightforward heat diffusion calculation, incorporating continuity of heat flow across the MnAs/GaAs interface, shows that the top and bottom MnAs interfaces have a temperature difference < 1 °C for $\tau > 100$ ns; hence, for later times heat diffusion in GaAs controls a nearly uniform MnAs temperature. For T_0 = 16 °C, δ initially drops as in Fig. 2(b) (not time-resolved with the cw probe) before attaining a maximum value at $\tau \sim 25$ ns, at which time the film has cooled to ~ 26 °C, where (see Fig. 1(b)) the maximum δ should occur; note, however, that the maximum δ is

not unity since a temperature-, and ξ–gradient is predicted from the diffusion model. For T_0 = 24 °C, the peak δ is delayed and occurs at $\tau \sim$ 100 ns, since the temperature (26 °C) for peak

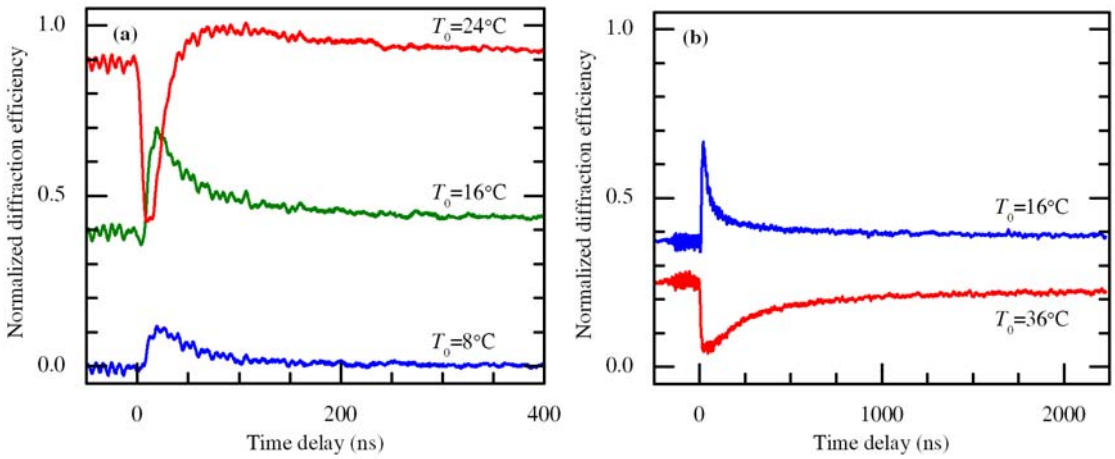

FIG. 3 (color online). (a) Time-dependent δ of a 409 nm probe for 150 nm thick MnAs at different T_0; a Φ pump pulse is used. (b) Same for T_0 = 16 and 36 °C but for longer times.

diffraction is now closer to the equilibrium temperature; the peak is also broader in time since $d\delta/dT_0$ is smaller (see Fig. 1(b)) as equilibrium is approached. For T_0 = 36 °C the peak in $\delta(\tau)$ is inverted since for higher temperatures δ is smaller than its equilibrium value. In all cases, for $\tau >$ 300ns, $\left[\delta(\tau)-\delta(\infty)\right] \propto \tau^{-p}$ with p = 0.54 ± 0.08 consistent with 1-D heat diffusion (p = 0.5).

For T_0 = 8 °C, Fig 3(a) shows that a transient striped phase with Λ ~ 750 nm begins at ~ 20 ns during cooling and lasts for ~ 75 ns. We find that a transient striped phase can be generated for T_0 as low as 4 °C, limited by sample damage at a fluence of ~ 9 mJcm^{-2}. The production of a transient coexistence phase likely requires sufficient energy to allow a significant portion of the film to reach a nearly uniform temperature above ~15 °C.

In summary, we have observed how strain-mediated domains evolve in MnAs thin films 150 fs to 2 μs after ultrashort pulse excitation. The elastic strain and α, β phase fractions oscillate while

the misfit strain declines on a nanosecond time scale through MnAs heat diffusion. Recovery of the equilibrium structure takes > 100 ns via heat diffusion in the substrate. For a film initially in the α-phase a transient coexistence phase occurs after ~ 10 ns during cooling. Although magnetization dynamics have not been needed to understand the main features observed here, magneto-elastic coupling likely forces the magnetization to evolve with local temperature and lattice constant, *i.e.*, following the phase diagram. The magneto-optical Kerr effect [36] is often used to study magnetization, but spatially inhomogeneous structural- and strain-dependent birefringence make it difficult to unambiguously separate magnetization and structural effects here. Nonetheless, our diffraction experiments [37] provide insight into domain structural dynamics in strained magnetic films. We expect similar nonequilibrium dynamics to occur in other ferroic and superconducting films.

We gratefully acknowledge Ken Burch for stimulating our interest in MnAs and Christoph Lange and Rashmi Desai for discussion of some of the results. UT work was supported by the Natural Sciences and Engineering Research Council of Canada; work at PSU was partially supported by NSF DMR 0801406.

*vandriel@physics.utoronto.ca

……..

[1] G. Catalan, J. Seidel, R. Ramesh and J.F. Scott, Rev. Mod. Phys. **84**, 119 (2012).

[2] J.H. Haeni *et al*., Nature **430**, 758 (2004).

[3] V. M. Kaganer, B. Jenichen, F. Schippan, W. Braun, L. Däweritz, and K. H. Ploog, Phys. Rev. Lett. **85**, 341 (2000).

[4] P. Sharma *et al*., Nat. Mat. **2**, 673 (2003).

[5] S.G. Han, Z.V. Vardeny, K.S. Wong, O.G. Symko and G. Koren, Phys. Rev. Lett., **65**, 2708 (1990).

[6] N. Sridhar, M. Rickman, and D.J. Srolovitz, Acta. Mater. **44**, 4085 (1996).

[7] N. Sridhar, M. Rickman, and D.J. Srolovitz, Acta. Mater. **44**, 4097 (1996).

[8] A.L. Roytburd, J. Appl. Phys. **83**, 228-38 (1998).

[9] A.L. Roytburd, J. Appl. Phys. **83**, 239-245 (1998).

[10] R.C. Desai and R. Kapral, *Dynamics of Self-organized and Self-assembled Structures*, (Cambridge), (2009).

[11] F. Heusler, Z. Ang. Chem. **1**, 260 (1904).

[12] C. P. Bean and D.S. Dodbell, Phys. Rev. **126**, 104 (1962).

[13] V. M. Kaganer, B. Jenichen, F. Schippan, W. Braun, L. Däweritz, and K. H. Ploog, Phys. Rev. B **66**, 045305 (2002).

[14] L. Däweritz, Rep. Prog. Phys. **69**, 2581 (2006).

[15] Y. Takagaki, C. Herrmann, J. Herfort, C. Hucho, and K.-J. Friedland, Phys. Rev. B**78**, 235207 (2008).

[16] R. Breitwieser, F. Vidal, I. L. Graff, M. Marangolo, M. Eddrief, J.-C. Boulliard, and V. H. Etgens, Phys. Rev. B**80**, 045403 (2009).

[17] A. M. Lindenberg, *et al*., Phys. Rev. Lett. **84**, 111 (2000).

[18] M. Forst, C. Manzoni, S. Kaiser, Y. Tomioka, Y. Tokura, R. Merlin, and A. Cavalleri, Nat. Phys. **7**, 854-856 (2011).

[19] S. Wall, D. Wegkamp, L. Fogia, K. Appavoo, J. Nag, R.F. Haglund, J. Stahler and M. Wolf, Nat. Comm. **3**, 721 (2012).

[20] N. Gedik, D.-S. Yang, G. Logvenov, I. Bozovic, and A.H. Zewail, Science **316**, 425 (2007).

[21] G. Ju, J. Hohlfeld, B. Bergman, R. J. M. van de Veerdonk, O. N. Mryasov, J.-Y. Kim, X.Wu, D. Weller, and B. Koopmans, Phys. Rev. Lett. **93**, 197403 (2004).

[22] J.-Y. Bigot, M. Vomir, and E. Beaurepaire, E., Nat. Phys. **5**, 515-520 (2009).

[23] B. Vodungbo, *et al*., Nat. Com. **3**, 999 (2012).

[24] R. Lu, M. Hase, M. Kitjama, S. Nakashima and S. Sugai, Phys. Rev. B **75**, 012107 (2007).

[25] B. Gallas, J. Rivory, H. Arwin, F. Vidal, and V. H. Etgens, Phys. Stat. Sol. (a) **205,** 859 (2008).

[26] M.Born and E. Wolf, *Principles of Optics*, 5th Edition (Pergamon) (1975).

[27] K. Bärner, R. Braunstein, and E. Chock, Phys. Stat. Sol.(b), **80**, 451 (1977).

[28] M. Dörfler and K. Bärner, Phys. Stat. Sol. (a) **17**, 141 (1973).

[29] One might surmise that $\delta(\tau)$ should oscillate with twice the frequency of an elastic wave, *i.e*., the diffraction *energy* efficiency should be maximal twice for every full oscillation cycle. However, as indicated in the figures the entire film is never transformed into the β–phase (except when $T_0 \geq 36\,^{\circ}\mathrm{C}$) and perhaps only minimally below a certain depth. The amplitude of the surface grating is therefore the sum of oscillating and constant terms; unless the oscillating part were to dominate (with more than half the film thickness undergoing oscillations), the phase of the stripe oscillations does not reverse, and there will only be one diffraction oscillation for each strain wave oscillation.

[30] C. Thomsen, J. Strait, Z. Vardeny, H.J. Maris, J. Tauc, and J.J. Hauser, Phys. Rev. Lett. **53**, 989 (1984).

[31] M. K. Liu, *et al.,* Phys. Rev. Lett. **107**, 066403 (2011).

[32] S. Fujieda, Y. Hasegawa, A. Fujita, and K. Fukamichi, J. Appl. Phys., **95**, 2429 (2004).

[33] J.-W. Schünemann, A. Lange, G.A. Govor, K. Bärner, and E. Gmelin, J. Alloys and Cmpds., **178**, 237 (1992).

[34] J. Hohfield, Chem. Phys. **251**, 237 (2000).

[35] J.S. Blakemore, J. Appl. Phys. **53**, R123 (1982).

[36] Z. Q. Qiu and S.D. Bader, Rev. Sci. Instr. **71,** 1243 (2000).

[37] While our data was being analyzed Sacchi *et al*. [M. Sacchi, C. Spezzani, E. Allaria, E. Ferrari, M. Coreno, M. Marangolo, M. Eddrief, V. Etgens, and G. De Ninno, Appl. Phys. Lett. **100**, 211905 (2012).] reported similar pump-probe diffraction experiments on a T_0 = 34 °C, 300 nm MnAs film using 150 fs, 130 nm probe, and 390 nm pump, pulses but only for $\tau < 100$ ps. They observe a monotonic *decrease* of δ in ~ 15 ps, which they suggest might reflect a decrease of ξ. For T_0 = 36 °C we observe an *increase* in δ for ~5 ps followed by oscillatory behavior. Without knowing all their experimental parameters, including temperature and wavelength dependence, we do not wish to speculate on the interpretation of their results. Our focus also is only on domain dynamics at longer times and for films with several values of ξ.